

# Optimization of anti-reflection layer and back contact of Perovskite solar cell

Najmedin Shahverdi<sup>a,\*</sup>, Maryam Yaghoubi<sup>b</sup>, Mahdi Goodarzi<sup>c</sup>, Ali Soleamani<sup>d</sup>

<sup>a</sup> Department of Electronic Engineering, Borujerd Branch, Islamic Azad University, Borujerd, Iran

<sup>b</sup> Department of Electronic Engineering, Mahshahr Branch, Islamic Azad University, Mahshahr, Iran

<sup>c</sup> Department of Electronic, Afarinesh Institute of Higher Education, Borujerd, Iran

<sup>d</sup> Department of Electrical and Robotics Engineering, Shahrood University of Technology, Shahrood, Iran

## ARTICLE INFO

### Keywords:

Graphite connector  
Device simulation  
Silvaco  
Perovskite solar cells  
Anti-reflection layer

## ABSTRACT

A perovskite-based solar cell is a solar cell introduced in recent years. One of its obvious weaknesses is its low efficiency, which makes it possible to consider this type of solar cell in multiple (paired) forms with a solar cell of the other type. The CIGS and a-si and c-si solar cells are typical examples paired with perovskite solar cells to increase efficiency. The efficiency of 28% was achieved without the presence of a pair of other types by changing some parameters such as the thickness of the absorbent layer and the right choice of the anti-reflection layer and the back contact layer.

To investigate the effect of the anti-reflection layer on the efficiency of Perovskite solar cells, materials such as Al<sub>2</sub>O<sub>3</sub>, SiO<sub>2</sub> and ZnO with various thicknesses were placed as an anti-reflection layer, with the best efficiency achieved by SiO<sub>2</sub> with an optimum value of 100 nm. Graphite connector was also considered as an optimal choice because the inexpensiveness and flexibility of this material compensate for a 2% reduction in efficiency.

This study shows that solar cell can be constructed based on the only perovskite, which represents a new generation of cheap and economical solar cells, which are very easy to construct and their raw materials are very accessible. The numerical simulation tool used in this study was the Silvaco software atlas module. The J-V specification is simulated under the standard AM 1.5G lighting.

## 1. Introduction

The crystalline silicon solar cells (c-si) have long dominated the photovoltaic market, accounting for about 90% of the market share (Fischer et al., 2012). However, the power conversion efficiency (PCE) of the crystalline silicon solar cell has remained constant over the past 15 years. The efficiency of 25.6% has been achieved for the silicon device recently (Masuko et al., 2014), and this value was limited to 29% for single crystal silicon (c-si) solar cells (Richter et al., 2013). Also, optimal solar energy production requires reducing the cost of designing and installing photovoltaic cells (Powell et al., 2012). Therefore, low-cost solar cells are needed to get the proper conversion efficiency and lower costs. The organic-mineral halide Perovskite solar cells (PSCs) have entirely changed the condition.

In 2009, Teshima et al. used ( ) and (CH<sub>3</sub>NH<sub>3</sub>PbBr<sub>3</sub>) as an adsorbent in solar cells, yielding the efficiency values of 3.81% and 3.13%, respectively (Kojima et al., 2009). Many other studies have been conducted to improve the performance of the Perovskite solar cell. In 2015,

the approved efficiency was 20.1 percent (Yang et al., 2015). Recently, efficiency above 22.7% has been obtained (Jeon et al., 2018). Several methods have been developed to improve the performance of Perovskite solar cells, such as composite engineering, solvent engineering, and interfacing engineering (Chang et al., 2016; Li et al., 2017; Wang et al., 2017; Liu et al., 2018; Zhang et al., 2018). Perovskite has an appropriate bandgap of 1.55 e.v, a sharp optical absorption edge with a below-the-bandgap absorption (De Wolf et al., 2014), and a high absorption coefficient (Leguy et al., 2015).

Improving the photoelectric efficiency of solar cells is an important issue that scientists have been trying to solve for a long time. One of the critical factors that affects the efficiency of solar cells is the reflection of light-emitting light to the surface of the solar cell. In order to reduce the reflection loss, a single or multilayer anti-reflection layer is usually placed on the surface of the solar cell. The anti-reflection layer plays an important role in increasing the efficiency of solar cell transformation, because it can cause light to appear in the active parts of the device. The anti-reflection layer is usually made of one or several layers of dielectric

\* Corresponding author.

E-mail address: [elec.faraz@gmail.com](mailto:elec.faraz@gmail.com) (N. Shahverdi).

<https://doi.org/10.1016/j.solener.2019.07.040>

Received 5 May 2019; Received in revised form 5 July 2019; Accepted 11 July 2019

0038-092X/ © 2019 International Solar Energy Society. Published by Elsevier Ltd. All rights reserved.

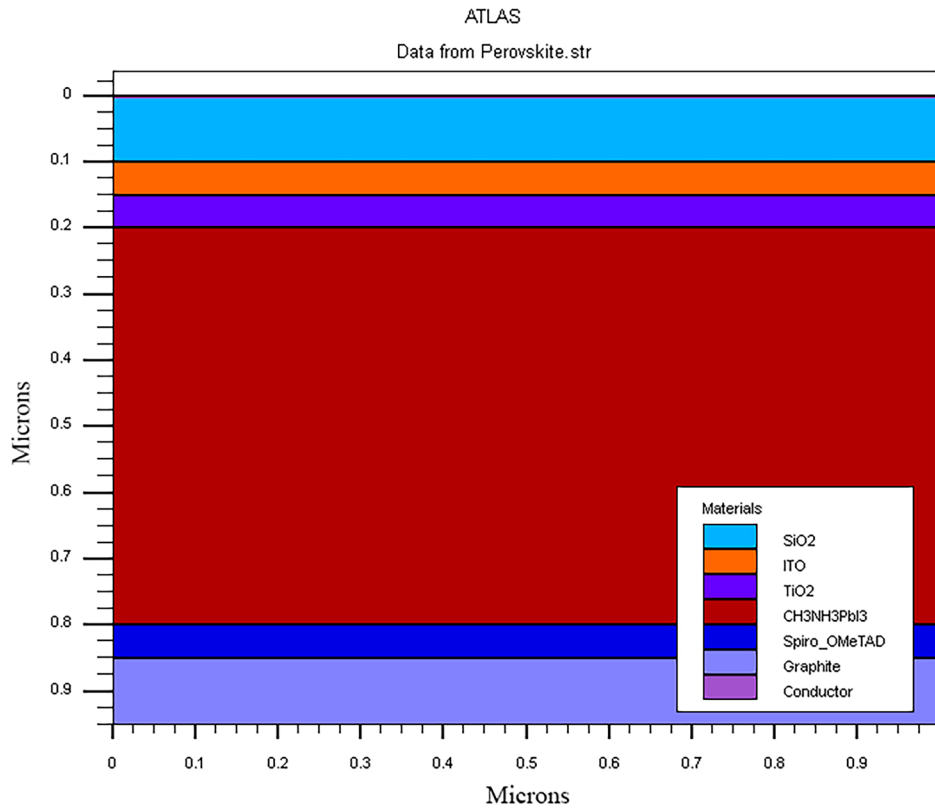


Fig. 1. Physical structure of Perovskite solar cell.

(non-conductive). Its thickness is a quarter of the wavelength of the light, and, due to the interference phenomenon, it reduces the reflection (Takato et al., 1992; Doshi et al., 1997; Aberle, 2001; Orgassa et al., 2002; Ramanathan et al., 2003; Richards, 2004). Anti-reflection layers can also be of the type of nano-porous films or woven films that have the advantage of trapping light for greater bandwidth response (Kennedy and Brett, 2003; Richards et al., 2003; Jaysankar et al., 2018). There are many reports that focus on the design and production of anti-reflection layers. Peng Zhao et al. obtained the best results from aluminum oxide (Al<sub>2</sub>O<sub>3</sub>) by analyzing several elements as an anti-reflection layer (Zhao et al., 2018). Hence, we decided to place other materials such as SiO<sub>2</sub> and ZnO as an anti-reflection layer, with the highest efficiency achieved with SiO<sub>2</sub>.

One of the best and unique features of a Perovskite solar cell is its flexibility. Replacing gold or silver metal as a back contact of Perovskite solar cell, which reduces the flexibility of this cell, has always been one of the challenges of this type of solar cell. In this paper, we have made it more economical by introducing the graphite, which is one of the carbon derivatives, instead of gold or silver, in addition to increasing the flexibility of the Perovskite solar cell.

## 2. Simulation

The Silvaco software atlas simulator was used in this study to identify and investigate the effects of changes in the material type and the thickness of the anti-reflection layer and the back contact on the performance of Perovskite solar cells. This simulation is essentially based on three main equations: Poisson's equation, load-continuity equation, and the drift-diffusion model:

Poisson's equation:  $\frac{\partial^2 \phi}{\partial x^2} = \frac{q}{\epsilon}(n - p)$   
 The continuity equations for electrons and holes:  
 $\frac{\partial n}{\partial t} = \frac{1}{q} \frac{\partial J_n}{\partial x} + G - R$ ,  $\frac{\partial p}{\partial t} = -\frac{1}{q} \frac{\partial J_p}{\partial x} + G - R$   
 $J_n$  and  $J_p$  are explained by the drift-diffusion model:  
 $J_n = qD_n \frac{\partial n}{\partial x} - q\mu_n n \frac{\partial \phi}{\partial x}$ ,  $J_p = -qD_p \frac{\partial p}{\partial x} - q\mu_p p \frac{\partial \phi}{\partial x}$

$\phi$ : Electric potential  $\epsilon$ : the permittivity  $q$ : charge of an electron  $n, p$ : the electron and hole concentrations  $J_n, J_p$ : The electron and hole current densities  $G, R$ : generation (recombination) rates for the electrons and holes  $D_n, D_p$ : Electron and Hole constant diffusion  $\mu_n, \mu_p$ : Electron and Hole mobility's

Device simulation enables us to identify the fundamental physical phenomenon occurring in a solar cell, and as a result, we can validate estimates about the optimal conditions for optimal solar cell performance.

Fig. 1 shows the physical structure of the Perovskite solar cell. The top-down proximity-based solar cell components according to Fig. 1 are:

- The anti-reflection layer; we examined several different materials such as Al<sub>2</sub>O<sub>3</sub> (Kumar et al., 2009), SiO<sub>2</sub> (Palik, 1998), ZnO (ElAnzeery et al., 2015) in this layer, and the optimum thickness for this layer was found to be 100 nm, as explained in Section x.
- A layer of indium tin oxide (ITO); this layer is used with a thickness of 50 nm and as a transparent connector in this solar cell; silence index and refractive index (n, k) for this layer are extracted from (Holman et al., 2013).
- A layer of titanium dioxide (TiO<sub>2</sub>) (Cui et al., 2016) is considered as an electron transfer material (buffer) with a thickness of 50 nm.
- The primary layer of this solar cell is the layer known as Perovskite, which consists of a combination of several organic-inorganic halides (PSCs), Methylammonium lead iodide (CH<sub>3</sub>NH<sub>3</sub>PbI<sub>3</sub>) and is used as an absorbent layer. The silence index and refractive index (n, k) for this layer are extracted from (Loper et al., 2015).
- The most common material used as a hole transducer (buffer) in Perovskite solar cells is the Spiro-OMeTAD polymer composition. The properties of this composition, including the appropriate glass transition temperature, solubility, ionization potential, and transparency in the range of visible spectra, have made it a convenient option for photovoltaic applications. The thickness of this layer is

**Table 1**  
Parameters of Perovskite Solar Cell Simulation.

Parameter	Anti-reflection	ITO	TiO2	CH3NH3PbI3	Spiro_OMeTAD	Back connector Graphite	Back connector Graphite
Thickness (nm)	100	50	50	600	50	400	400
$N_A$ ( $\text{cm}^{-3}$ )	–	–	–	$2 \times 10^{14}$	–	–	–
$N_D$ ( $\text{cm}^{-3}$ )	–	–	–	–	$1 \times 10^{17}$	$2 \times 10^{14}$	–
Resistivity	100	100	100	30	10	100	100
chi	0	0	0	4.58	4.18	4.17	–
$E_g$ (eV)	–	–	–	1.07	2.48	1.08	0
$N_C$ ( $\text{cm}^{-3}$ )	–	–	–	$2.5 \times 10^{18}$	$2.5 \times 10^{18}$	$1 \times 10^{20}$	–
$N_V$ ( $\text{cm}^{-3}$ )	–	–	–	$2.5 \times 10^{19}$	$1 \times 10^{20}$	$1 \times 10^{19}$	–

$N_A$  ( $\text{cm}^{-3}$ ): Acceptor Concentration,  $N_D$  ( $\text{cm}^{-3}$ ): Donor Concentration,  $N_C$  ( $\text{cm}^{-3}$ ): Effective Conduction Band Density,  $N_V$  ( $\text{cm}^{-3}$ ): Effective Valence Band Density,  $E_g$ : bandgap energy, chi: Electron dependency, resistivity: Electric resistance is in Table 1.

also considered 50 nm. The refractive index and refractive index (n, k) for this layer have been extracted from (Filipič et al., 2015).  
f. back contact layer; that in this study, we used several materials such as Gold (Johnson and Christy, 1972), Aluminum (Johnson and Christy, 1972), Graphite (Phillip and Taft, 1964), and Copper (Johnson and Christy, 1972) to achieve better efficiency for Perovskite solar cells. Section 3 explains the results in detail.

In the simulation, the Transmission Matrix (TMM) method was used as an optical model for calculating carrier production rates. SRH recombining models, radiation recombination and Auger combinations are considered. The standard AM 1.5G solar spectrum is used to obtain the voltage-current density diagram (J-V) under the lighting [35]. The electrical parameters that we used for Perovskite solar cells in the

simulation are summarized in Table 1.

### 3. Results and discussion

#### 3.1. The effect of changing the thickness of the perovskite adsorbent layer (CH3NH3PbI3) on Perovskite solar cell

One of the parameters affecting the efficiency of a Perovskite solar cell is the thickness of its absorbent layer. In order to fully investigate the effect of the back contact on the operation of the solar cell, it is first necessary to obtain the optimal thickness of the Perovskite layer (CH3NH3PbI3).

We considered the back contact of gold in this section. Figs. 2–4 show an increase in absorbent layer thickness versus quantum

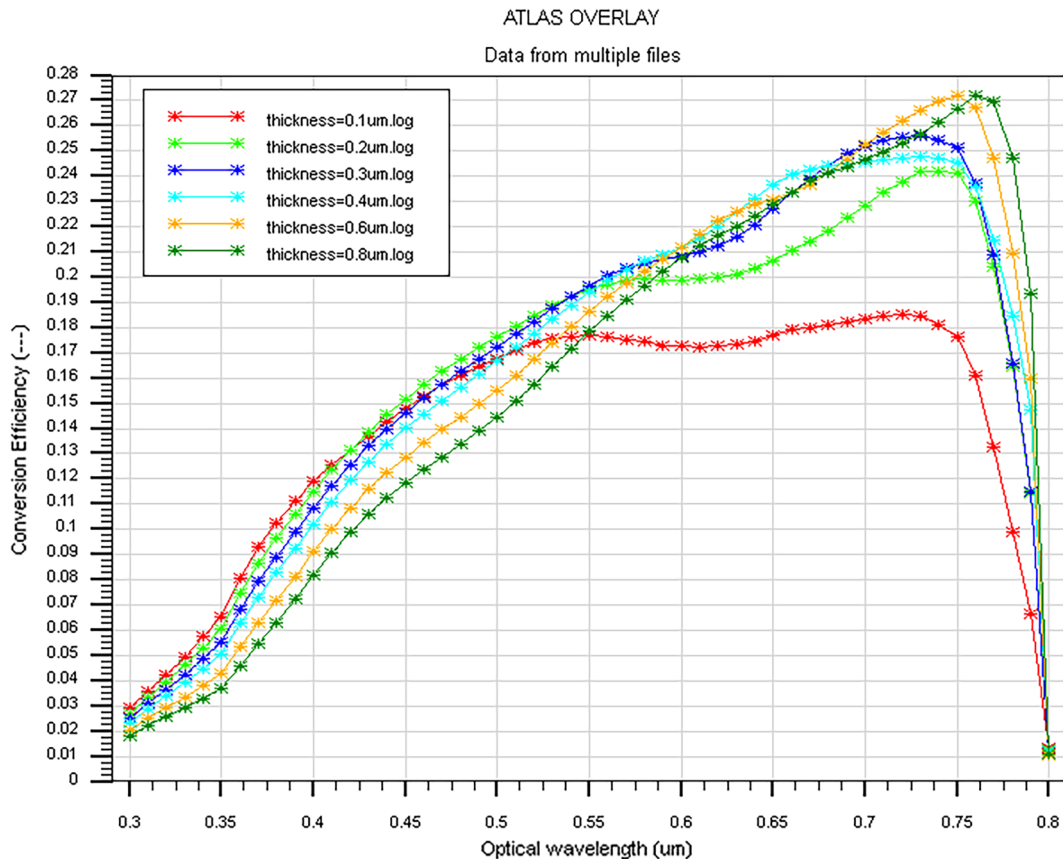


Fig. 2. Effect of thickness change of Perovskite layer (CH3NH3PbI3) on Perovskite solar cell efficiency.

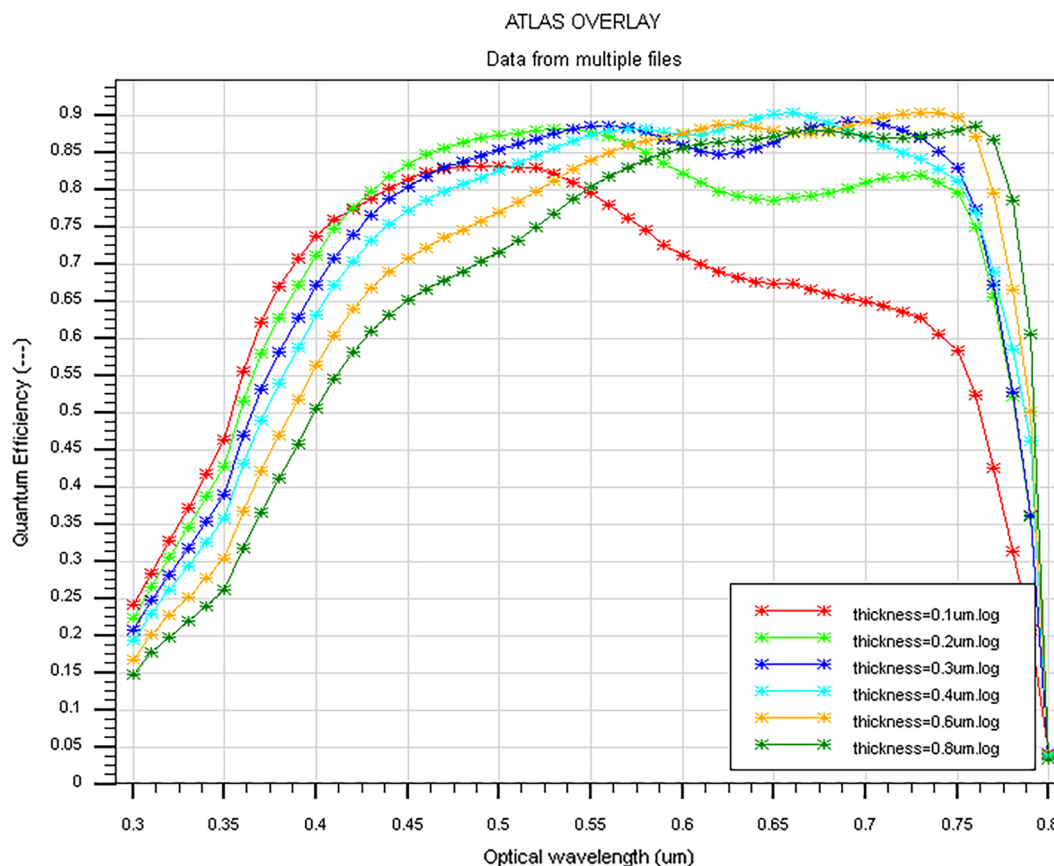


Fig. 3. The effect of thickness change of the Perovskite layer ( $\text{CH}_3\text{NH}_3\text{PbI}_3$ ) on the quantum efficiency of Perovskite solar cell.

efficiency and light reflection. It can be seen that an increase in the thickness of the Perovskite layer leads to an increase in the efficiency, but an increase up to 600 nm for the absorbent layer will increase the efficiency to 27%. Afterward, following an increase in the thickness of the Perovskite layer, the efficiency will not increase and the amount will remain constant. Finally, we conclude that the best results are obtained for a thickness of 600 nm absorbent layer.

Fig. 4 shows absorption in the Perovskite solar cell. According to this figure, the lowest light absorption for a thickness of 200 nm was obtained for the  $\text{CH}_3\text{NH}_3\text{PbI}_3$  layer. It is normal to increase the absorption of light by increasing the thickness of the absorption layer. The highest light absorption occurs for light spectra whose wavelengths range from 400 to 750 nm.

### 3.2. Investigating the effect of anti-reflection layer on Perovskite solar cell efficiency

In this section, we put  $\text{SiO}_2$ ,  $\text{Al}_2\text{O}_3$ ,  $\text{ZnO}$  as an anti-reflection layer. As we can see from Figs. 5–7 and Table 2, the best and worst results were obtained for  $\text{SiO}_2$  and  $\text{ZnO}$ , respectively. This occurred because of the transparency of the  $\text{SiO}_2$  and  $\text{Al}_2\text{O}_3$  materials and the non-transparent nature of the  $\text{ZnO}$  substance. The presence or absence of this layer has a significant effect on the overall efficiency of the Perovskite solar cell.

This layer acts like a light trap, so that the direction of motion of light moves into the cell when the light enters the cell, because the light

emits from the outside into the cell (the first-order refractive index of the air is lower than the second-order refractive index of the anti-reflection layer). When the light is inside the solar cell, and intends to exit the cell (because the first-order refractive index of the first-layer anti-reflection layer is higher than the second medium that is the air), the light is reflected back into the first environment, and the light escape is prevented.

In Figs. 8–10, the anti-reflection layer is considered to be  $\text{SiO}_2$ , and its thickness is changed from 50 nm to 500 nm. It should be noted that for thicknesses less than 100 nm, an increase in the thickness of the anti-reflection layer leads to an increase in the efficiency parameters, quantum efficiency and light reflection in the solar cell, while for thicknesses larger than 100 nm, such an increase in the thickness of the anti-reflection layer leads to a decrease in the efficiency parameters, quantum efficiency, and light reflection in a solar cell.

This shows that the optimum thickness for the anti-reflection layer is 100 nm. This is clear for thicknesses smaller than 100 nm (as shown in Fig. 8), but the reason for thicknesses greater than 100 nm is that the spectrum affecting the Perovskite solar cell is from 200 nm to 800 nm. Moreover, if the thickness of this layer exceeds the wavelength of the incoming wave, it prevents them from entering the cell.

### 3.3. Effect of several materials as a back contact on the performance of Perovskite solar cell

In Figs. 11–13 gold, aluminum, copper and graphite are located as

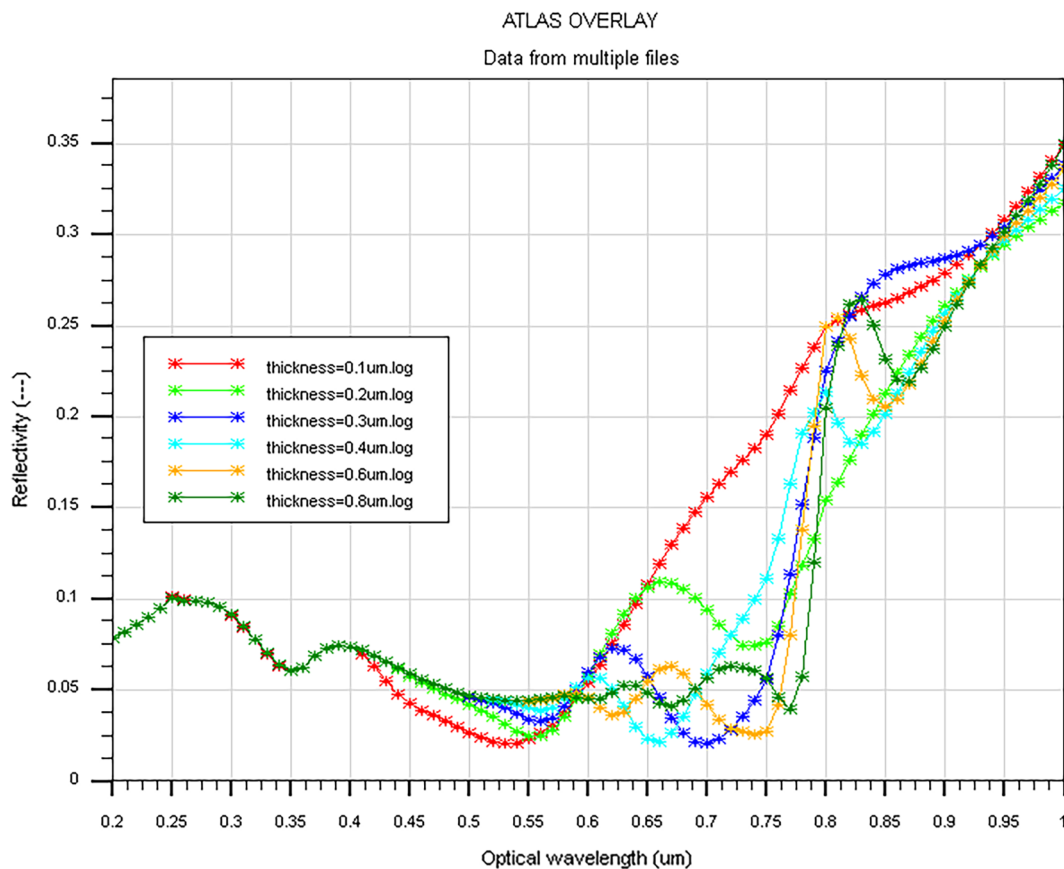


Fig. 4. Effect of thickness change of Perovskite layer (CH<sub>3</sub>NH<sub>3</sub>PbI<sub>3</sub>) on photonic reflection of Perovskite solar cell.

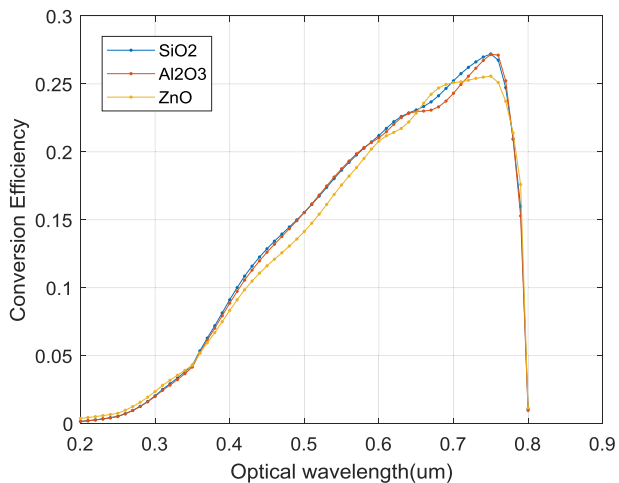


Fig. 5. Results of the use of SiO<sub>2</sub>, Al<sub>2</sub>O<sub>3</sub>, ZnO materials as an anti-reflection layer on Perovskite solar cell efficiency.

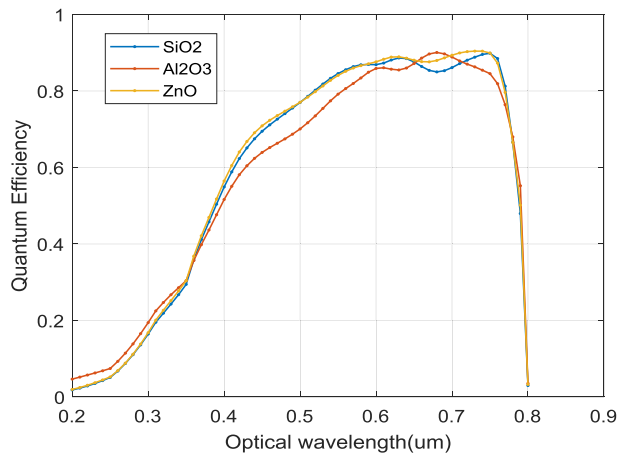


Fig. 6. Effects of the use of SiO<sub>2</sub>, Al<sub>2</sub>O<sub>3</sub>, ZnO materials as an anti-reflection layer on the quantum efficiency of Perovskite solar cell.

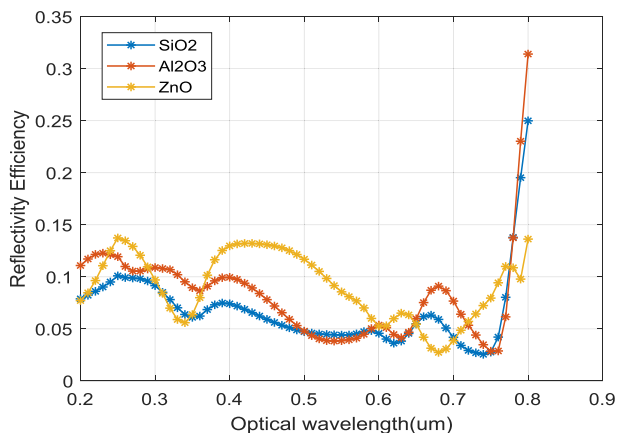


Fig. 7. Light reflection by SiO2, Al2O3, ZnO as an anti-reflection layer of Perovskite Solar Cells.

**Table 2**  
The effect of using different materials as an anti-reflection layer on Perovskite solar cell efficiency.

Wave length (nm)	SiO2	Al2O3	ZnO
710	25.75	24.96	25.16
720	26.22	25.57	25.27
730	26.62	26.15	25.41
740	26.98	26.73	25.50
750	27.20	27.18	25.57
760	26.75	27.12	25.11
770	24.73	25.23	23.72
780	20.93	20.94	21.39
790	15.98	15.28	17.60

back contacts. According to Table 3, the efficiency values of Perovskite solar cell for gold, aluminum, copper and graphite were 27.2%, 25.35%, 26.89%, 25.05% respectively, in the same conditions and thickness. Copper is preferred to gold due to the low difference in the results obtained for gold and copper metals in order to save money.

It should be noted that, according to Table 1, the type of graphite material was considered as a donor semiconductor with a carrier load concentration of  $2 \times 10^{14}$  atom/cm<sup>3</sup> and the remaining materials as conductive.

**4. Conclusion**

This study dealt with the effect of adsorption layer thickness (CH3NH3PbI3) on efficiency, quantum efficiency and light reflection. Thicknesses (100, 200, 300, 400, 600, 800) nm were selected for simulation for the adsorbent layer, which the best results obtained with a thickness of 600 nm. Then, SiO2, Al2O3, ZnO materials were placed as an anti-reflection layer, which gave SiO2 the highest efficiency for light with a wavelength of 750 nm. SiO2, Al2O3, ZnO materials were also placed as the anti-reflection layer, and the highest efficiency was obtained with SiO2 for a light with a wavelength of 750 nm. Finally, gold, aluminum, copper and graphite were tested as back contacts, and the best efficiency of 27.2% was obtained for gold back contact.

It is not definitely possible to determine which material is better for the back contact because the efficiency is reduced by 0.3% if gold is replaced by copper, but it makes the Perovskite solar cell fabrication process more cost-effective.

One of the promising features of Perovskite solar cell is its flexibility. If the graphite material were replaced instead of copper or gold metal, there would be a 15.2% reduction in efficiency compared to the gold connector. But the flexibility of the graphite material is better than all of the materials used as a back contact in this study.

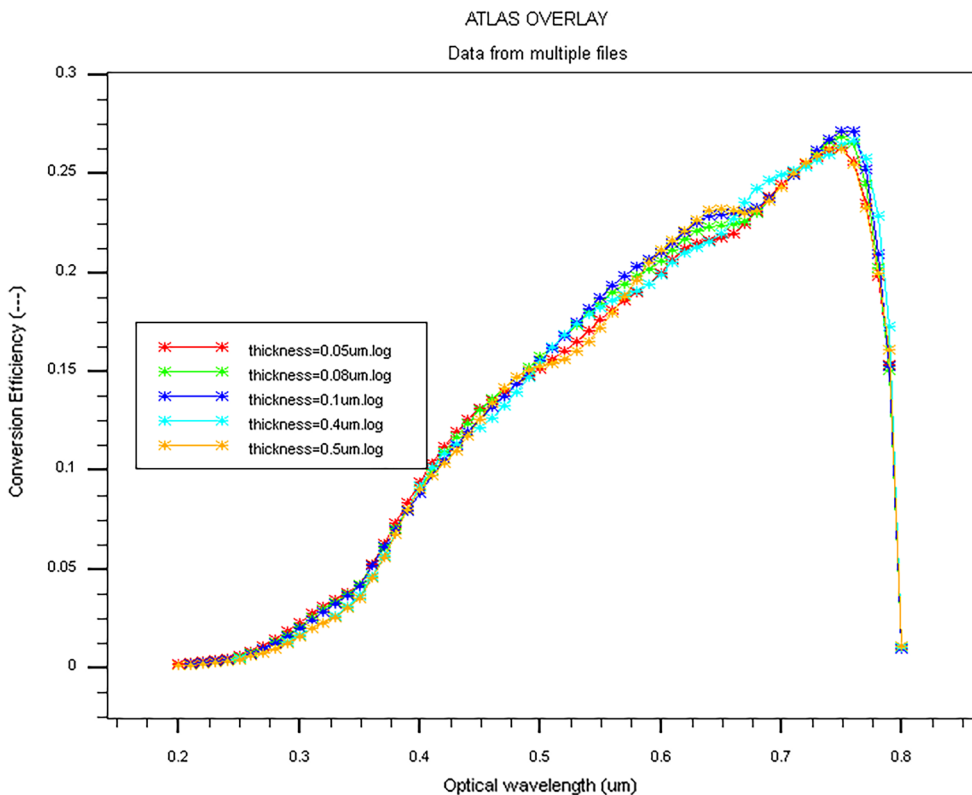


Fig. 8. The effect of the change in the thickness of the anti-reflection layer, SiO2, on the Perovskite solar cell efficiency.



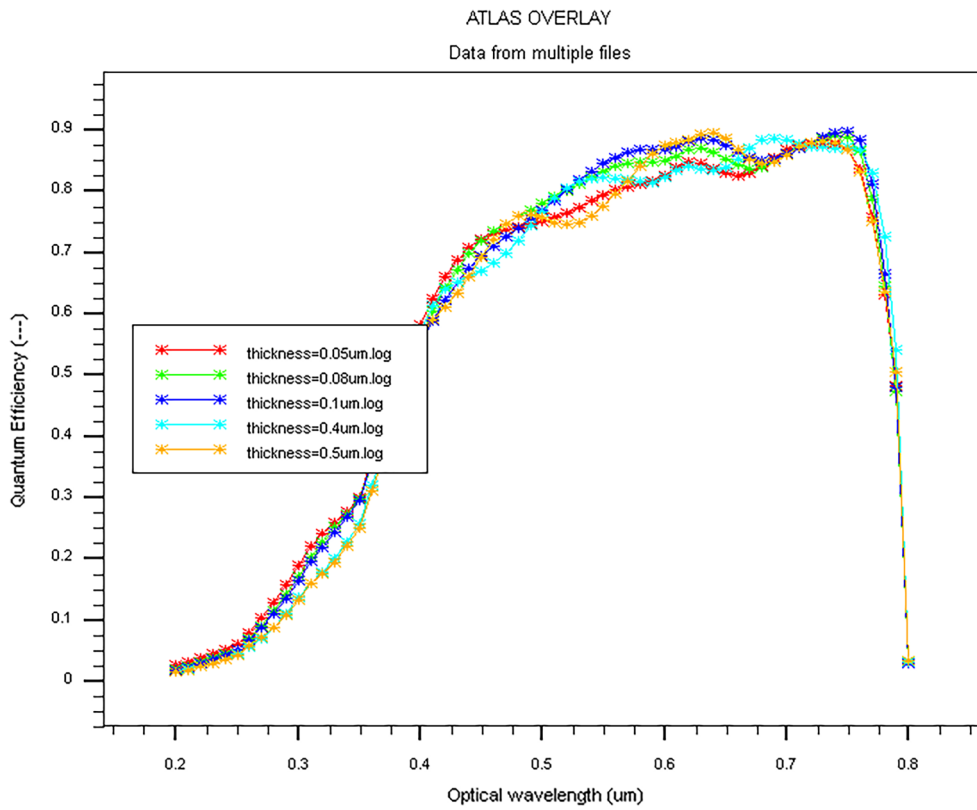


Fig. 9. The effect of changing the thickness of the anti-reflection layer, SiO<sub>2</sub>, on the quantum efficiency of Perovskite solar cell.

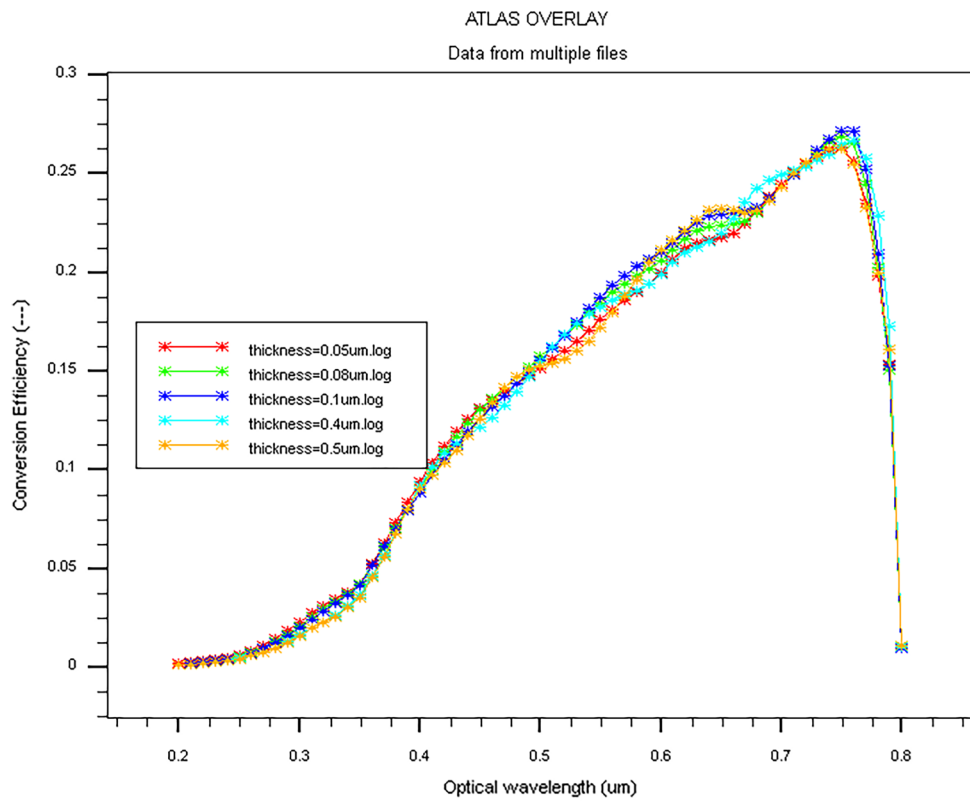


Fig. 10. The effect of the change in the thickness of the anti-reflection layer, SiO<sub>2</sub>, on the reflection of Perovskite solar cell.

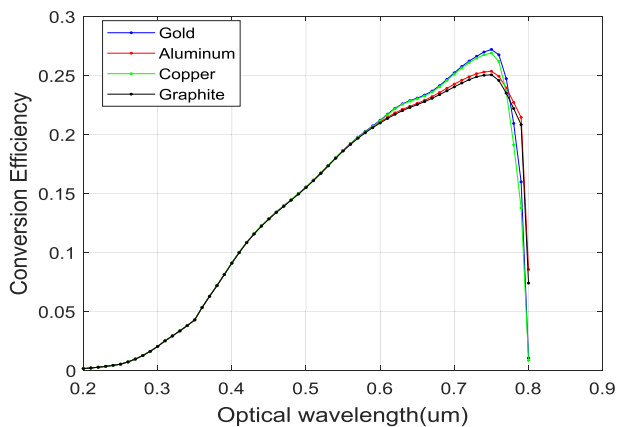


Fig. 11. The effect of different materials as a back contact on the efficiency of Perovskite solar cells.

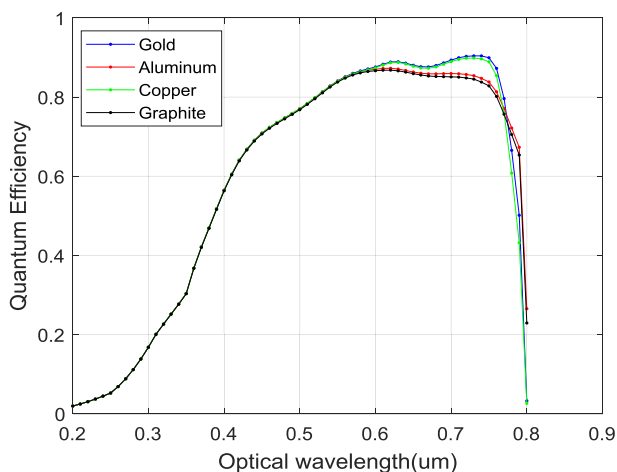


Fig. 12. The effect of different materials as a back contact on the quantum efficiency of Perovskite solar cell.

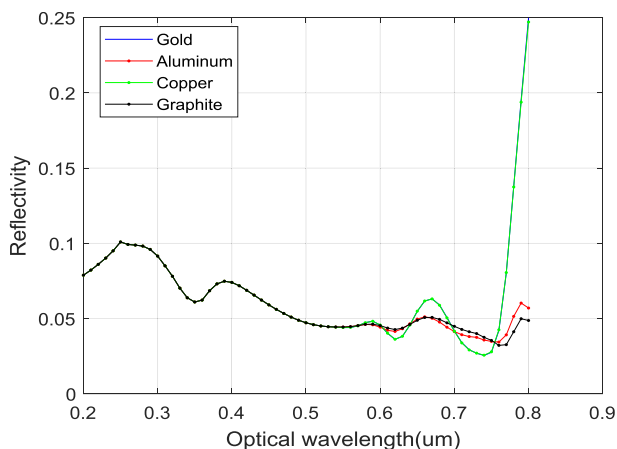


Fig. 13. The effect of different materials as a back contact on photon reflection in Perovskite solar cell.

**Table 3**  
The Effect of Different Materials as back contacts on the Efficiency of Perovskite Solar Cells.

Wavelength (nm)	Gold	Aluminum	Copper	Graphite
720	26.22	24.89	26.08	24.64
730	26.62	25.15	26.46	24.89
740	26.98	25.29	26.76	25.01
750	27.20	25.35	26.89	25.05
760	26.75	24.93	26.18	24.57
770	24.73	23.94	23.60	23.50
780	20.93	22.71	19.13	22.19
790	15.98	21.45	13.77	20.83
800	1.05	8.56	0.85	7.40

One of the challenges of Perovskite solar cells is the their lifespan uncertainty, for which it is hoped that a solution will be found in the next studies.

**Declaration of Competing Interest**

Conflict of interest On behalf of all authors, the corresponding author states that there is no conflict of interest.

**Appendix A. Supplementary material**

Supplementary data to this article can be found online at <https://doi.org/10.1016/j.solener.2019.07.040>.

**References**

Fischer, M., Metz, A., Raithel, S., 2012. Semi international technology for photovoltaics (ITRPV) challenges in C-Si technology for suppliers and manufacturers. In: 27th European Photovoltaic Solar Energy Conference and Exhibition, pp. 527–532.

Masuko, K., Shigematsu, M., Hashiguchi, T., Fujishima, D., Kai, M., 2014. Achievement of more than 25% conversion efficiency with crystalline silicon heterojunction solar cell. *IEEE J. Photovolt.* 4 (6), 1433–1435.

Richter, A., Hermle, M., Glunz, S.W., 2013. Reassessment of the limiting efficiency for crystalline silicon solar cells. *IEEE J. Photovolt.* 3 (4), 1184–1191.

Powell, D.M., et al., 2012. Crystalline silicon photovoltaics: a cost analysis framework for determining technology pathways to reach baseload electricity costs. *Energy Environ. Sci.* 5 (3), 5874–5883.

Kojima, A., Teshima, K., Shirai, Y., Miyasaka, T., 2009. Organometal halide perovskites as visible-light sensitizers for photovoltaic cells. *J. Amer. Chem. Soc.* 131 (17), 6050–6051.

Yang, W.S., et al., 2015. High-performance photovoltaic perovskite layers fabricated through intramolecular exchange. *Science* 348 (6240), 1234–1237.

Jeon, N.J., et al., 2018. A fluorene-terminated hole-transporting material for highly efficient and stable perovskite solar cells. *Nat. Energy* 3, 682–689.

Chang, J., et al., 2016. Enhancing the photovoltaic performance of planar heterojunction perovskite solar cells by doping the perovskite layer with alkali metal ions. *J. Mater. Chem. A* 4 (42), 16546–16552.

Zhang, R., et al., 2018. Theoretical lifetime extraction and experimental demonstration of stable cesium-containing tri-cation perovskite solar cells with high efficiency. *Electrochim. Acta* 265, 98–106.

Wang, Y., et al., 2017. Stitching triple cation perovskite by a mixed anti-solvent process for high-performance perovskite solar cells. *Nano Energy* 39, 616–625.

Li, S., et al., 2017. Interface engineering of high-efficiency perovskite solar cells based on ZnO nanorods using atomic layer deposition. *Nano Res.* 10 (3), 1092–1103.

Liu, Z., et al., 2018. High-performance planar perovskite solar cells using low temperature, solution-combustion-based nickel oxide hole transporting layer with efficiency exceeding 20%. *Adv. Energy Mater.* 8, 1703432.

De Wolf, S., et al., 2014. Organometallic halide perovskites: sharp optical absorption edge and its relation to photovoltaic performance. *J. Phys. Chem. Lett.* 5 (6), 1035–1039.

Leguy, A.M.A., et al., 2015. Reversible hydration of CH3NH3 PbI3 in films, single crystals, and solar cells. *Chem. Mater.* 27 (9), 3397–3407.

Ramanathan, K., et al., 2003. Properties of 19.2% efficiency ZnO/CdS/CuInGaSe2 thin-film solar cells. *Prog. Photovolt., Res. Appl.* 11 (4), 225–230.

Aberle, A.G., 2001. Overview on SiN surface passivation of crystalline silicon solar cells.



- Sol. Energy Mater. Sol. Cells 65 (1–4), 239–248.
- Takato, H., et al., 1992. Effects of optical confinement in textured antireflection coating using ZnO films for solar cells. *Jpn. J. Appl. Phys.* 31, L1665–L1667.
- Richards, B.S., 2004. Comparison of TiO<sub>2</sub> and other dielectric coatings for buried-contact solar cells: a review. *Prog. Photovolt., Res. Appl.*, 12 (4), 253–281.
- Orgassa, K., Rau, U., Nguyen, Q., Werner Schock, H., Werner, J.H., 2002. Role of the CdS buffer layer as an active optical element in Cu(In, Ga)Se<sub>2</sub> thin-film solar cells. *Prog. Photovolt., Res. Appl.*, 10 (7), 457–463.
- Doshi, P., Jellison, G.E., Rohatgi, A., 1997. Characterization and optimization of absorbing plasma-enhanced chemical vapor deposited antireflection coatings for silicon photovoltaics. *Appl. Opt.* 36 (30), 7826–7836.
- Kennedy, S.R., Brett, M.J., 2003. Porous broadband antireflection coating by glancing angle deposition. *Appl. Opt.* 42 (22), 4573–4579.
- Richards, B.S., Rowlands, S.F., Honsberg, C.B., Cotter, J.E., 2003. TiO<sub>2</sub> DLAR coatings for planar silicon solar cells. *Prog. Photovolt., Res. Appl.*, 11 (1), 27–32.
- Jaysankar, M., et al., 2018. Perovskite-silicon tandem solar modules with optimized light harvesting. *Energy Environ. Sci.* 11 (6).
- Zhao, P., et al., 2018. Device simulation of organic-inorganic halide perovskite/crystalline silicon four terminal tandem solar cell with various antireflection materials. *IEEE J. Photovoltaics* 8 (6), 1685–1691.
- Kumar, P., Wiedmann, M., Winter, C., Avrutsky, I., 2009. Optical properties of Al<sub>2</sub>O<sub>3</sub> thin films grown by atomic layer deposition. *Appl. Opt.* 48 (28), 5407–5412.
- Palik, E. (Ed.), 1998. *Handbook of Optical Constants of Solids*. Academic Press, Orlando pp. 759–0.
- ElAnzeery, H., El Daif, O., Buffière, M., Oueslati, S., Ben Messaoud, K., Agten, D., Brammertz, G., Guindi, R., Kniknie, B., Meuris, M., et al., 2015. Refractive index extraction and thickness optimization of Cu<sub>2</sub>ZnSnSe<sub>4</sub> thin film solar cells. *Phys. Status Solidi (a)* 212 (9), 1984–1990.
- Holman, Z., Filipic, M., Descoedres, A., De Wolf, S., Smole, F., Topic, M., Ballif, C., 2013. Infrared light management in high-efficiency silicon heterojunction and rear-passivated solar cells. *J. Appl. Phys.* 113 (1), 013107.
- Cui, J., Allen, T., Wan, Y., McKeon, J., Samundsett, C., Yan, D., Zhang, X., Cui, Y., Chen, Y., et al., 2016. Titanium oxide: a re-emerging optical and passivating material for silicon solar cells. *Sol. Energy Mater. Sol. Cells* 158, 115–121.
- Loper, P., Stuckelberger, M., Niesen, B., Werner, J., Filipic, M., Moon, S., Yum, J., Topic, M., De Wolf, S., Ballif, C., et al., 2015. Complex refractive index spectra of CH<sub>3</sub>NH<sub>3</sub>PbI<sub>3</sub> perovskite thin films determined by spectroscopic ellipsometry and spectrophotometry. *J. Phys. Chem. Lett.* 6, 66–71.
- Filipic, M., Loper, P., Niesen, B., De Wolf, S., Krc, J., Ballif, C., Topic, M., 2015. CH<sub>3</sub>NH<sub>3</sub>PbI<sub>3</sub> perovskite silicon tandem solar cells: characterization based optical simulations. *Opt. Express* 23 (7), A263–A278.
- Johnson, P.B., Christy, R.W., 1972. Optical constants of the noble metals. *Phys. Rev. B* 6, 4370–4379.
- Phillip, H.R., Taft, E.A., 1964. Kramers-kronig analysis of reflectance data for diamond. *Phys. Rev.* 136, A1445–A1448.